A Public Deep IRAC Survey in the Extended CDF−South

Principal Investigator: Pieter van Dokkum
Institution: Yale
Electronic mail: dokkum@astro.yale.edu
Co−Investigators: Pat McCarthy, Carnegie, Pasadena
Megan Urry, Yale
Hans−Walter Rix, MPIA, Heidelberg
Ivo Labbe, Carnegie, Pasadena
Marijn Franx, Leiden
Eric Gawiser, Yale
Jiasheng Huang, CfA
Niel Brandt, Penn State
Mark Dickinson, NOAO
Garth Illingworth, UC Santa Cruz
Casey Papovich, U of Arizona
Eric Bell, MPIA, Heidelberg
Paulina Lira, U de Chile
Sukyoung Yi, Oxford
Rychard Bouwens, UC Santa Cruz
Ned Taylor, Leiden
Danilo Marchesini, Yale
Science Catagory: Extra Galactic: Survey(s)
Observing Modes: IRAC Mapping
Hours Requested: 122.9

Abstract:
The 0.5 x 0.5 deg area surrounding the CDF−South is the only cosmological survey field that has multi−wavelength coverage from X−rays to the thermal infrared and whose size exceeds the correlation length of massive galaxies at $1<z<4$. More than 10,000 redshifts are known, ~800 AGN have been detected, and two−band HST ACS imaging exists over the whole field. While the GALEX, Chandra, HST, and MIPS data in this field are all very deep, the existing IRAC data are not. Deep IRAC data have been shown to be pivotal in a) identifying massive high

redshift objects, b) estimating galaxy masses, and c) completing the census of AGN and their host galaxies. Hence we propose deep public IRAC imaging across the whole Extended CDF−South to enable such analyses over a large enough area where the evolution of cosmic average properties can be well measured. The full set of Great Observatories data in this 900 square arcmin low−background field offers unparalleled archival value for future studies with ALMA and 20m−30m telescopes.

A Public Deep IRAC Survey in the Extended CDF-South

1. Background

Recent years have seen great progress in our understanding of galaxy formation and evolution, as large telescopes on the ground and in space have opened up the high redshift Universe for research. We can select candidate galaxies out to $z \sim 7$ from ground- and space-based images and confirm them spectroscopically (e.g., Bouwens et al. 2004; Ouchi et al. 2005), allowing systematic study of the properties of galaxies when the Universe had less than 10 % of its present age. The best studied high redshift population are the Lyman break galaxies (LBGs), selected by the strong discontinuity blueward of the far-UV Lyman limit (e.g., Steidel et al. 1999).

The rapid progress has also high-lighted areas where our understanding is still lacking, and where new information is most urgently needed. Building on previous work on "Extremely Red Objects" (EROs), deep near-infrared imaging surveys have uncovered substantial populations of red, presumably massive, galaxies at $2 < z < 4$, which are underrepresented in samples selected by the Lyman break technique (Franx et al. 2003, van Dokkum et al. 2003, Daddi et al. 2003; Yan et al. 2004). These UV-faint galaxies could dominate the stellar mass budget at $z \sim 3$ and yet had gone undetected until very recently. Furthermore, an as yet unknown fraction of star forming galaxies at early epochs is heavily obscured by dust (e.g., Blain et al. 2002), making it very difficult to identify them in the optical or even the near-IR. It has also become apparent that AGN may play an important role in the evolution of normal galaxies, as black hole mass correlates tightly with properties of their host galaxies (e.g., Kormendy & Gebhardt 2001). The hard X-ray sources found by Chandra presumably pinpoint the progenitors of today's supermassive black holes in the centers of bulges and ellipticals, but the fact that many are very faint in the optical has hampered efforts to understand these objects and their host galaxies (Brandt & Hasinger 2005, and refs therein). Finally, it has now become clear that strong clustering leads to dramatic variations in the inferred number density and properties of massive galaxies measured in small fields. Structures of several tens of Mpc have been found up to $z \sim 6$ (e.g., Ouchi et al. 2005), underscoring the importance of sampling large volumes at high redshift.

The field of galaxy formation has taken a major step forward with the advent of deep imaging surveys with MIPS and IRAC on Spitzer. IRAC allows selection of normal galaxies out to $z \sim 3$ in the rest-frame near-IR rather than the rest-frame UV or optical, which is much closer to a selection by stellar mass. Furthermore, the high sensitivity and efficient mapping modes of Spitzer make it feasible to execute surveys over sufficiently large areas to suppress cosmic variance and to *measure* the clustering of distant populations rather than being limited by it. As the Spitzer photometry alone is seldom sufficient to unambiguously identify and characterize sources (see, e.g., Yan et al. 2004) it is critical that such mapping projects are done in areas which have the best possible observations at other wavelengths – and are optimal fields for ALMA. This proposal aims to take the next crucial step beyond the GOODS Legacy program by providing deep, public IRAC imaging in the Extended CDF-South: a $0.5^\circ \times 0.5^\circ$ low-background region of the sky with by far the best supporting data of any field of comparable area.

2. The rich data in the Extended CDF-South

The low-background $0.5^\circ \times 0.5^\circ$ "flanking field" of the GOODS CDF-S Legacy area (the Extended CDF-South, or E-CDFS) has by far the best multi-wavelength data currently available or scheduled

in *any* field of comparable or larger size. Apart from the usual complement of very deep ground based *UBVRI* imaging (from ESO and the Yale/Chile MUSYC Survey) and extensive multi-object spectroscopy (from COMBO-17, LCIRS, VIMOS/GOODS and MUSYC), the field has a unique suite of supporting datasets.

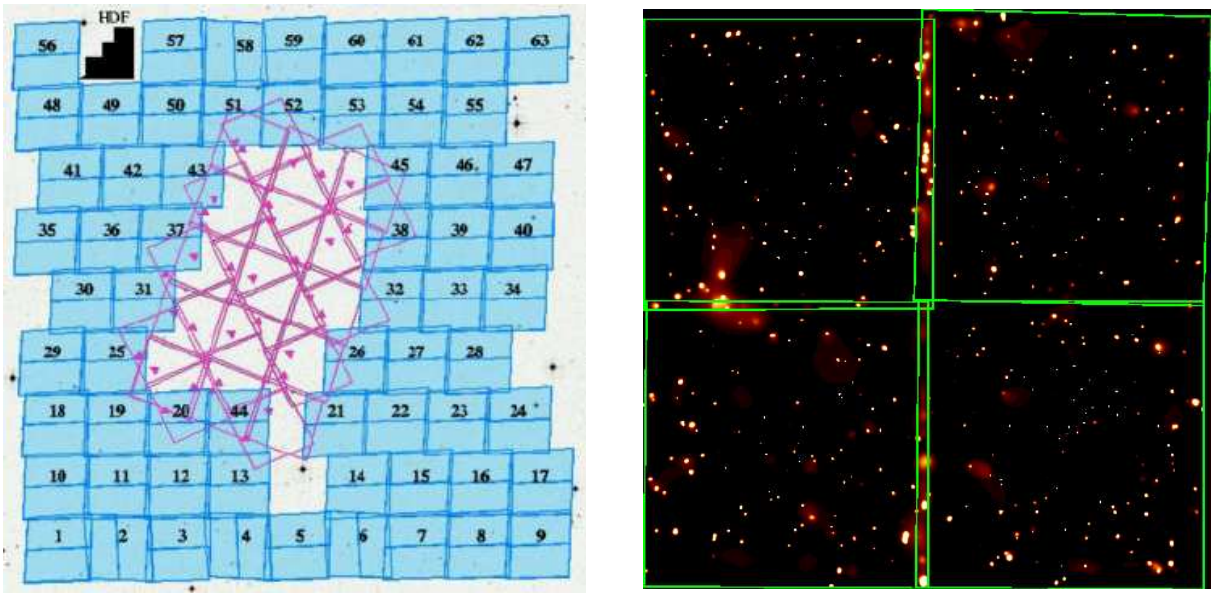

Fig. 1. The $0.5^\circ \times 0.5^\circ$ Extended CDF-South (E-CDFS), as observed with HST (left; PI Rix) and Chandra (right; PI Brandt). There are 880 X-ray sources in the Chandra mosaic, of which ~ 770 are AGN. In the center of the field is the CDF-South itself, which is also the GOODS South Spitzer Legacy field. We propose to augment the existing deep HST, Chandra, XMM, GALEX, MIPS, and ground-based data in the E-CDFS with public IRAC images.

• **HST ACS imaging in two bands over the whole field.** A mosaic of 78 ACS pointings from GEMS (Rix et al. 2004) reaches 5σ AB depths of 28.3 in F606W and 27.1 in F850LP (Fig. 1).

• **Chandra, XMM, and radio data.** In its largest survey after the Chandra Deep Field campaigns, Chandra imaged the whole E-CDFS with an exposure time of 250 ks per pixel (PI: Brandt), augmenting the 1 Ms Chandra Deep Field data in the center. There are 880 X-ray sources in these exquisite Chandra images; about ~ 770 of these are AGNs, with the remainder powerful star burst galaxies. Furthermore, a 540 ks XMM observation covers ~ 70 % of the ECDF, and ATCA is surveying the E-CDFS at 1.4 GHz to a 5σ depth of 50 μJy.

• **Deep MIPS data.** The GTO MIPS imaging in the E-CDFS is among the deepest outside of the GOODS region, reaching a depth of $\sim 80\,\mu$Jy at 24 micron. As discussed below these deep data are not well matched to the existing 500 s IRAC exposures of the GTO team; this proposal aims to increase the IRAC exposure time by a factor of ~ 20.

• **HST parallel fields.** Simultaneous with the exposures for the GOODS and Ultra Deep Field programs an equal number of parallel observations was obtained with NICMOS, STIS, WFPC2, and ACS, which mostly fall outside the GOODS area. These parallels represent some of the deepest UV, optical and NIR images ever taken.

• **Ultra-deep GALEX imaging.** With 44.7 ks of exposure time in the near- and far-UV the E-CDFS is currently the deepest public GALEX field; additional exposures totalling 200 ks are planned over the 1° GALEX field.

• **Deep near-infrared imaging.** By combining two substantial survey efforts, the LCIRS (McCarthy et al. 2001) and the Yale/Chile MUSYC survey (Gawiser et al. 2005), the E-CDFS has the deepest *JHK* imaging available over any $0.5^\circ \times 0.5^\circ$ field. The combined data reach a 5σ depth of $K_{\rm AB} = 22.5$ over the full area. Obtaining such deep NIR data is very expensive in terms of telescope time, but has proven to be of critical importance for interpreting Spitzer data: near-IR images provide both accurate source identifications and bridge the large wavelength gap between UV/optical data and the Spitzer bandpasses (see, e.g., Labbé et al. 2005).

• **Redshifts for** $10,000$ **galaxies to** $R = 24$**.** The field is the primary COMBO-17 field, a medium-band filter survey that has yielded accurate redshifts ($\sigma(z) \approx 0.02$) for 10,000 galaxies to a limit of $R = 24$. Apart from their obvious intrinsic value, these redshifts (together with spectroscopic redshifts) serve to calibrate broad-band photometric redshifts of fainter sources.

For all major imaging instruments *with the exception of Spitzer/IRAC*, the data obtained in the E-CDFS are the most comprehensive over any $0.5^\circ \times 0.5^\circ$ field. We propose to complete the multi-wavelength coverage in this field by increasing the IRAC exposure time by a factor of ~ 20. We emphasize that this field is a premier choice for a large public survey with Spitzer because of its low background. Like the E-CDFS, the (equatorial) COSMOS and UKIDSS fields are accessible from Chile. However, the Zodiacal background light is a factor of two higher in these fields, and to reach the same depth in the IRAC filters the integration times would have to be a factor of four higher.

3. Science36 137 577 655

A wide range of science programs will be enabled by the proposed public survey, as has been the case with previous public surveys with HST, Chandra, and Spitzer. Furthermore, the full Great Observatories dataset in the E-CDFS will have lasting archival value into the era when HST, Spitzer, and Chandra are no longer operational, providing a premier field for follow-up studies with ALMA, JWST, and 20m-30m telescopes.

3.1. The Mass Assembly of Galaxies

In the standard hierarchical paradigm of galaxy formation (e.g., Kauffmann et al. 1993), galaxies started out small and were built up through many generations of mergers. Testing hierarchical formation has proven to be a difficult task, largely because of the difficulty connecting the (observed) evolution of the luminosity of galaxies to the (predicted) evolution of their dark matter. A major step towards testing galaxy formation theory is to measure the evolution of stellar *mass*, rather than luminosity (see, e.g., Dickinson et al. 2003; Rudnick et al. 2003). Thanks to Spitzer, robust measurements of the evolution of the stellar mass content of galaxies are now within reach.

The $8.0\,\mu$m IRAC band samples the rest-frame $K-$band at $z \sim 3$, allowing us to measure the evolution of the rest-frame K-band luminosity function (LF) over $\sim 85\,\%$ of the history of the Universe. With three hours of integration time we can detect galaxies with $M_K < -22$ at $z = 2.5$ (see Technical Section). Lyman break galaxies have $M_{V,*} = -23.0$ (Shapley et al. 2001) and $(V-K)_{\rm AB} \sim 1$, which implies that we sample the luminosity function down to $\sim M_* + 2$ at $z = 2.5$.

The rest-frame K-band is a much better estimator of stellar mass than optical bands, as it is less susceptible to the presence of luminous young stars (which may dominate the light but contribute little to the mass) and to dust extinction. Using a combination of deep optical, near-IR, and IRAC data in the HDF-South Labbé et al. (2005) show that the M/L ratios of $z \sim 2.5$ galaxies vary by a factor of ~ 25 in the rest-frame V band, and only a factor of ~ 6 in rest-frame K. M/L_K ratios of the $8\,\mu$m selected sample can be determined from fits to the full restframe UV to near-IR

spectral energy distributions (see, e.g., Dickinson et al. 2003; Labbé et al. 2005). The near-infrared *JHK* imaging in the E-CDFS is of particular importance in this context as these filters sample the redshifted Balmer- and 4000 Å breaks for $1.5 < z < 3$. The M/L_K ratios can be used to convert the observed rest-frame *K* luminosity function to a mass function.

Redshifts for a subset of the 8.0 μm selected objects will already be available from COMBO-17, the ESO/GOODS public redshift survey, and the other campaigns listed in § 2. Furthermore, we plan extensive spectroscopic follow-up of the 8.0 μm selected sample using our access to Magellan, the VLTs, Gemini, and Keck (with the obvious efficiency advantage of having GOODS and the UDF in the center of the field). The redshifts serve to calibrate broad band photometric redshifts determined from the full GALEX+HST+*UBVRIJHK*+IRAC+MIPS photometry.

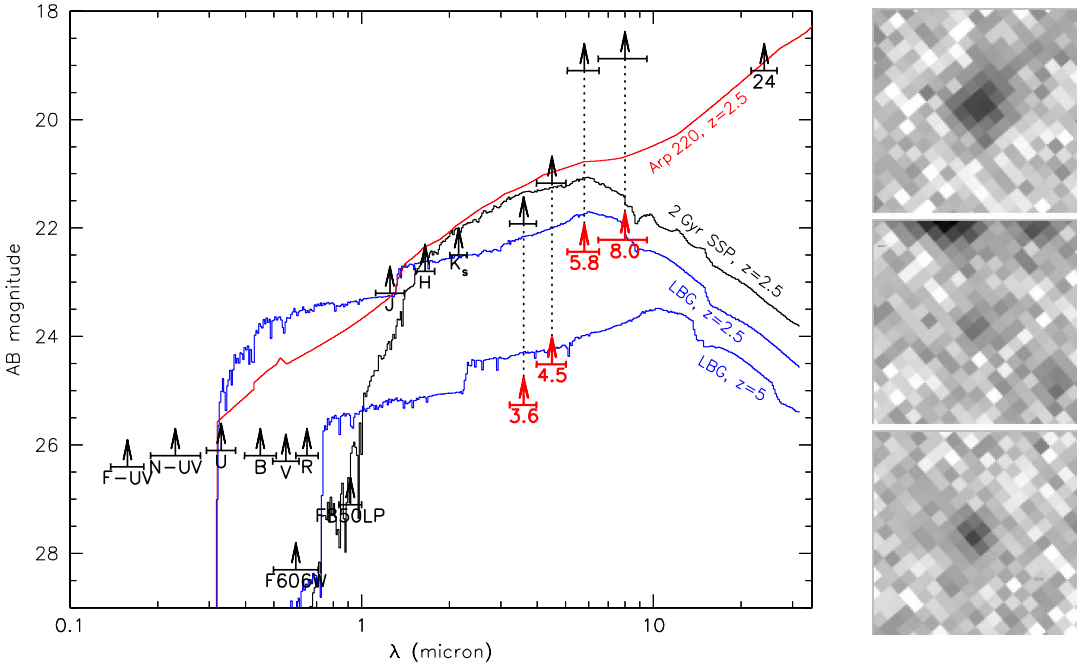

Fig. 2. *Left:* Current 5σ limits from 0.15 – 24 μm in the E-CDFS along with the much deeper IRAC limits that would result from the present proposal. The curves show SEDs for different galaxy types at a fixed redshift of $z = 2.5$, and the SED for an L_* LBG at $z = 5$. *Right:* IRAC 3.6 μm images of three $z \sim 5$ galaxies in the UDF, with $\mathrm{F850LP_{AB}} \approx 25.5$ and a range of optical – mid-IR colors, degraded to the S/N of the proposed observations. The proposed IRAC observations allow selection and study of galaxies to $z \sim 5$ at 3.6/4.5 μm and to $z \sim 3$ at 3.6 – 8.0 μm, and are well matched to the available data at other wavelengths.

3.2 IRAC Properties of MIPS Sources

From the initial analyses of deep MIPS images it has become clear that deep IRAC observations are critical to understand the 24 μm-selected population: the higher resolution of the IRAC images is needed to identify the sources, and the shorter wavelength data help to determine the emission mechanism of the MIPS-selected sources. MIPS probes re-radiated dust emission, which can come from a deeply embedded star burst, an AGN, or a combination. As shown by Stern et al. (2005) IRAC photometry can distinguish between these possibilities, as the re-radiated dust does not contribute to the short-wavelength IRAC bands.

The MIPS GTO team has obtained deep coverage of the entire E-CDFS at 24, 70, and 160 μm: the 24 μm observations probe galaxies with IR luminosities $> 10^{11} L_\odot$ at $z \sim 1$ and $> 10^{12} L_\odot$ at $z \sim 2$ (Papovich et al. 2004). As shown in Fig. 2, the proposed IRAC depths enable accurate photometry of MIPS-detected dusty galaxies and AGNs.

3.3. Active Galactic Nuclei

Approximately $30-40\,\%$ of X-ray selected AGN are optically faint ($I > 24$; e.g., Alexander et al. 2001), and a subset of these remains undetected even in deep HST images (Koekemoer et al. 2004). These sources represent an important component ($> 20\,\%$) of the XRB and strongly overlap with the ERO and very red galaxy populations (Alexander et al. 2002; Barger et al. 2002). The majority are thought to be obscured AGN and QSOs at $z = 1-3$, although a high redshift tail is also expected to $z > 6$. Recently, the GOODS team has demonstrated that all X-ray sources in the CDF-South are bright in the IRAC passbands, including the seven that are undetected with HST (Treister et al. 2004; Koekemoer et al. 2005), lending strong support to the idea that they are highly obscured by dust.

There are 770 X-ray selected AGN in the E-CDFS, enabling us to extend the initial studies in the GOODS field to a ~ 4 times larger sample. The full photometric dataset in E-CDFS will provide strong constraints on the redshifts, masses, and stellar populations of the host galaxies. The $8\,\mu$m data will allow the study of potential hot dust components in low-to-moderate redshift AGN (many of which will be too faint to detect with MIPS). The large sample allows us to examine correlations between these parameters; of particular interest are the correlation between X-ray luminosity and degree of obscuration (see, e.g., Treister et al. 2004), and the relation between bolometric AGN luminosity with stellar mass of the host galaxy.

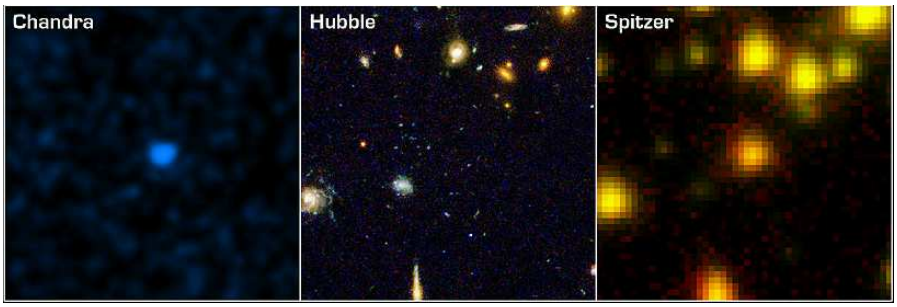

Fig. 3. Chandra, HST/ACS, and IRAC images of an X-ray selected AGN in the GOODS field (from Koekemoer et al. 2004, 2005). Many of these objects are faint or even undetected in optical passbands, but all are bright in the mid-IR.

3.4. Mid-IR Photometry of Normal Galaxies at $1 < z < 6$

• *Extremely Red Objects at* $1 < z < 2$

EROs are objects with red optical–near-IR colors, usually selected on the basis of $I-H$ or $I-K$. Their redshifts fall in the range $z = 1-2$, and initial discrepancies regarding their number density turned out to be caused by their strong clustering (Daddi et al. 2000). Interestingly a large fraction of the population appear to be obscured star forming galaxies, that may contribute significantly to the star formation rate at $z \sim 1$ (e.g., Smail et al. 2002). Dust emission starts to contribute to the SEDs of dusty starbursts beyond $1.6\,\mu$ in the restframe, which makes it possible to separate starbursting and normal galaxies in the ERO population using the 5.8 and $8.0\,\mu$ bands. As the ECDF is the primary area of the LCIRS survey (McCarthy et al. 2001) we have already identified a sample of ≈ 500 EROs with $K < 21$ and $I-K > 4.5$ in this field.

• *Red Galaxies at* $2 < z < 3$

Using the near-IR color criterion $J-K > 2.3$ we recently uncovered a population of galaxies with normal rest-frame optical colors beyond $z = 2$ that are too faint and red to be selected as LBGs

(Franx et al. 2003; van Dokkum et al. 2003). The optical–near-IR SEDs of these objects resemble those of normal spirals in the nearby Universe. Recent ERO samples selected with IRAC (I-EROs; Yan et al. 2004) have similar surface density, colors, and redshift range, and are likely the same population. Stellar mass estimates from IRAC observations in the HDFS indicate that at the high-mass end ($> 5 \times 10^{10} M_{\odot}$) the red galaxies contribute 80 % to the stellar mass budget at $z \sim 2.5$ (Labbé et al. 2005).

The rest-frame near-IR data from IRAC are critical for discriminating whether the red colors are caused by dust obscured star formation or evolved stellar populations; at their median $z \sim 2.5$ the $5.8\,\mu - 8.0\,\mu$ color is blue for SEDs dominated by evolved stars, and red for SEDs dominated by obscured star formation (see Fig. 2). The surface density of red galaxies is still uncertain, but based on the small fields studies so far, we expect to find ~ 700 in the ECDF at $K_{\rm AB} < 22.5$ (corresponding to $> 10\sigma$ photometry in all IRAC bands).

• *Luminous Galaxies at $z = 5 - 6$*
Studies of deep multi-color HST/ACS images have demonstrated that star forming galaxies can be selected by the Lyman break technique out to $z \sim 6$ (Bouwens et al. 2004; Dickinson et al. 2004). From optical and near-IR data alone it is very difficult to determine the physical properties of these galaxies, as they only sample the rest-frame ultraviolet. IRAC samples the SEDs redward of the Balmer break, allowing constraints on their ages and dust content. Although the GOODS survey is very well suited for studying large samples of these high redshift galaxies, most objects in the GOODS region are too faint for spectroscopic follow-up and confirmation. There are only ~ 10 luminous $z = 5 - 6$ objects with $\mathrm{F850LP_{AB}} < 25$ in GOODS, whereas there are $40 - 50$ in the 900 arcmin^2 E-CDFS. As illustrated in Fig. 2, they will be detected at $> 10\sigma$ in the 3.6 and 4.5 μ bands if they have similar SEDs to $z \sim 3$ LBGs. These luminous objects are important as they can be confirmed spectroscopically, and studied in much more detail than their faint counterparts. Furthermore, they are likely the seeds of today's massive galaxies in groups and clusters, and the combination of the deep GOODS survey and the wide survey proposed here can be used to determine whether a correlation between age and luminosity already existed at $z \sim 5$.

4. The need for a large area public survey

Our public IRAC survey is similar to the GTO IRAC deep survey. However, this survey is taken in the North on a field not accessible to ALMA, and lacks a comparable breadth of supporting observations. The proposed public survey complements the GOODS Legacy survey, which covers a much smaller area. Increasing the area is very important:

• It is becoming clear that the progenitors of massive galaxies were already highly clustered at early epochs: the correlation length of the most massive galaxies at $1 < z < 4$ is $\sim 10 h^{-1}$ comoving Mpc (e.g., Daddi et al. 2000, Adelberger et al. 2005). For massive galaxies at these redshifts the increase in area will reduce the uncertainties in measurements of both their clustering and their space densities by approximately a factor of two (Somerville et al. 2004).

• Bright high redshift galaxies and AGN are rare, and the larger area allows us to sample the bright end of the LF better than is possible within the GOODS regions. As an example, there are only five QSOs with $L_X > 3 \times 10^{44}$ ergs^{-1} s^{-1} in the CDF-South; similarly, there is only one $z \sim 6$ candidate in the GOODS field with $z_{F850LP} < 25$ (and only five with $z_{F850LP} < 25.5$). These bright objects are very important as they will suffer the least from confusion and have the best photometry at all wavelengths. Only for these objects is it likely that we can obtain detailed information on their nature, in particular from spectroscopy.

Technical plan

1. Observing strategy

We propose to image the $0.5° \times 0.5°$ Extended CDF-S with IRAC in all four bands. The field has a unique set of space- and groundbased supporting observations, including 78 deep HST/ACS pointings in two bands (PI: Rix), four 250 ks deep Chandra observations (PI: Brandt), and deep MIPS imaging. The observing strategy is dictated by the need to 1) cover the full field in all four bands; 2) avoid the ultra-deep GOODS area in the center of the field, and 3) achieve these goals for the large range of position angles that the field might be observed at.

The optimal solution is to tile the annulus around the GOODS area with units of 2×3 pointings in "mapping" mode. Each of these 2×3 units will produce a $10' \times 10'$ field with uniform coverage in all four bands, regardless of orientation. The 2×3 units will be spaced $5'$ apart to fill the entire annulus. The position angle will either be in the range $60° - 100°$ or in the range $200° - 240°$, depending on the observing window that will be chosen by the schedulers. The proposed pointing scheme is shown in Fig. 4, for two position angles: $80°$ and $220°$.

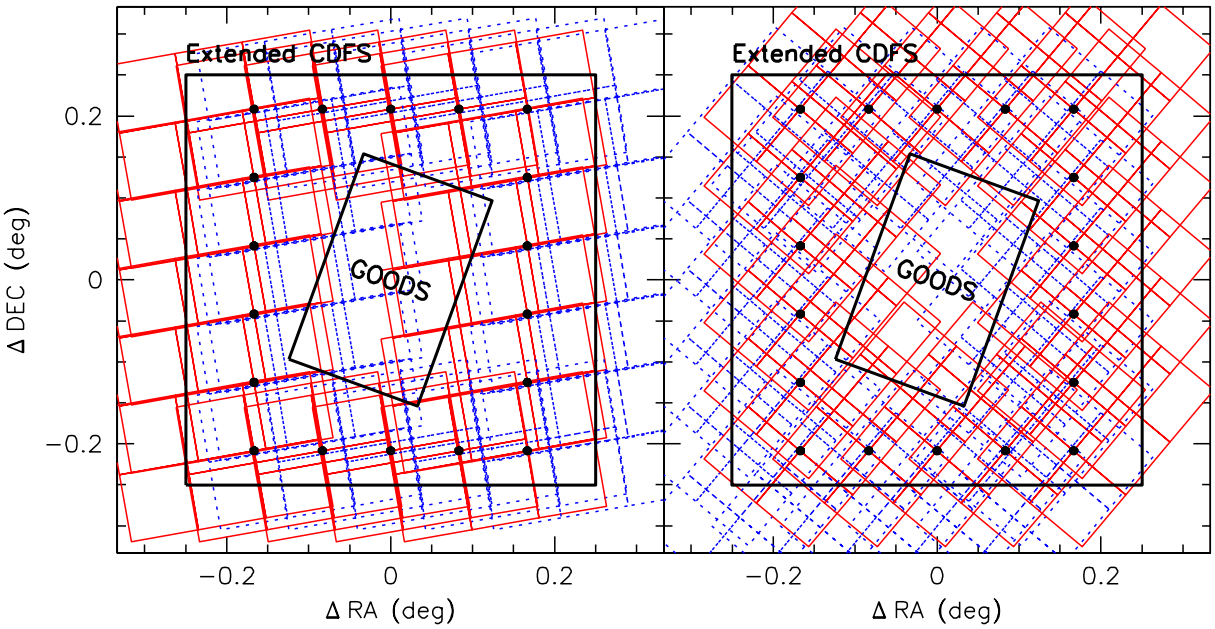

Fig. 4. Proposed field layout. Solid/red lines indicate the 4.5/8.0 μ FOV, and broken/blue lines the 3.6/5.8 μ FOV. Black dots indicate the centers of individual 2×3 tiles. With 18 tiles spaced $5'$ apart we can cover the entire ECDF (excluding the ultra-deep GOODS Legacy area) in all IRAC filters, with fairly uniform coverage. Each pixel will typically be covered by three different tiles. The two panels show typical roll angles for the Aug/Sept observing window (left) and the Jan/Feb observing window (right).

This pointing strategy optimizes the overlap with our large body of supporting data and avoids duplications in the ultra-deep GOODS area. Some small overlap with GOODS cannot be avoided; this redundancy is very useful as it allows us to assess the reliability of faint source detections in our data.

The integration time is 1 hour per pointing, i.e., 6 hrs for each 2×3 unit. We use medium-scale cyclic dithering, with 36 dither positions for each 1 hr pointing. For position angles near $220°$ each pixel will be covered by three different tiles, and the final coverage is nearly uniform at 3 hrs per pixel (right panel of Fig. 4). For position angles near $80°$ the coverage is 3 hrs over ~ 70 % of the

field, and 2 hrs over the remaining $\sim 30\,\%$. We note that fully uniform coverage for any position angle is not possible, and this is the best compromise.

The final exposure time is the same as that of the GTO deep survey in the North (the "Extended Groth Strip"), a factor of ~ 20 longer than the GTO program in the E-CDFS (PI G. Rieke, pid 81), and a factor of 8 shorter than the $10' \times 16'$ GOODS coverage (PI M. Dickinson, pid 194). It is therefore "mid-way" between the large area MIPS/IRAC GTO survey and the deepest extragalactic survey that Spitzer will likely undertake. Still, the proposed depth enables us to reach $M_* + 2$ for galaxies out to $z \sim 2.5$, and M_* to $z \sim 5$ (see Science Justification). Furthermore, this depth is well matched to the extensive multi-wavelength dataset in the E-CDFS, including the MIPS 24 μm imaging.

The integration time comfortably meets the requirement of achieving at least a factor three higher sensitivity than the GTO observations. A comparison is given in Table 1. These values do not take confusion into account, which starts to set in at short wavelengths for these exposure times. However, we stress that we will not *select* samples in the $3.6/4.5\,\mu$m bands, and (as has been demonstrated by the GOODS team) accurate photometry of sources selected at other wavelengths is feasible well below the nominal confusion limits. As discussed in 2.2 below, we will follow the GOODS strategy of subsampling the PSF and modeling the Spitzer sources using our deep HST/ACS images: this should achieve a factor of ~ 4 better S/N than possible with the GTO data even at $3.6/4.5\,\mu$.

Sensitivities (1σ; μJy)

	current (GTO)	proposed
$\sigma\,(3.6\,\mu)$	0.27	0.06
$\sigma\,(4.5\,\mu)$	0.54	0.12
$\sigma\,(5.8\,\mu)$	3.58	0.77
$\sigma\,(8.0\,\mu)$	4.38	0.94
Time (s)	500	10,800

2. Data analysis plan

2.1 Post-processing

As the depth of the planned exposures is substantial we expect that a significant amount of post-pipeline processing will be necessary to fully take advantage of the capabilities of IRAC. Taking the Basic Calibrated Data as a starting point, we will identify and remove subtle effects that only become apparent after adding several hours of data. Post-processing involves improving the flat fielding using the large number of dithered exposures, removing stray light caused by bright sources, possible bias drift, and other effects. Overlap regions between pointings will be used to calibrate the distortions and detector response in a self-consistent manner. Furthermore, pointings that partially overlap with the GOODS area will be used to calibrate our flat fielding procedures and near-confusion limited photometry (see below). Members of our team have extensive experience in optimally reducing very deep imaging data, and direct experience with IRAC. We envision an open exchange with the GOODS Legacy team and the GTO teams to ensure that all these datasets will be optimally processed.

2.2 Confusion-limited photometry

The deep IRAC observations in the $3.6\,\mu$ and $4.5\,\mu$ bands will be influenced by confusion effects. Confusion is not a hard limit, but largely influences the counts. For isolated sources, the GOODS

team has found that the noise decreases as $1/\sqrt{t}$ all the way to the GOODS limit. Furthermore, the GOODS team has done extensive simulations which show that it is possible to do accurate photometry beyond the nominal confusion limit even in crowded areas. The GOODS method (which we will adopt as part of our analysis) comprises the following: 1) creating subsampled images and PSFs by extensive, non-integer dithering; and 2) modeling the IRAC sources using the known positions of sources in deep HST/ACS images, leaving the IRAC flux as the only free parameter in a least-squares fit.

2.3 Data products

All data will be immediately public. In the spirit of the Legacy programs we will also provide the final reduced mosaic and catalogs to the community.

2.4 Team and distribution of tasks

Our team has extensive experience with multi-wavelength surveys and managing relatively large programs. Members of the team are Principal Investigators on various key programs in the ECDF: Hans-Walter Rix leads the GEMS HST/ACS imaging, Niel Brandt the ECDF Chandra imaging survey, Pat McCarthy the LCIRS near-IR survey, and Pieter van Dokkum the Chile/Yale MUSYC survey. Mark Dickinson, Jiasheng Huang, and Ivo Labbé have extensive experience with deep IRAC observations. Casey Papovich has extensive experience with MIPS, and will help tie the IRAC and MIPS data together. The team will be able to rapidly integrate the IRAC observations with the other ground- and space-based datasets in the ECDF.

Principal reduction and analyis work will be done at Yale, and data products will be available from a Yale web server. The science programs will be focussed at Yale (50 %: project management; red galaxies at $z > 2$; AGN), Carnegie (10 %: EROs and red galaxies), Penn State (10 %: AGN), UC Santa Cruz (10 %: $z \sim 5$ galaxies), NOAO/University of Arizona (10 %: MIPS/IRAC integration), Heidelberg (10 %: morphologies). Following JPL guidelines, no support is requested for the Heidelberg component; Rix and Bell and their students are fully supported from other sources.

Financial contact:

Dr. Suzanne K. Polmar
Director, Grant & Contract Admin.
Yale University, 155 Whitney Ave, PO Box 208337, New Haven, CT 06520-8337.

References

Adelberger, K., et al., 2005, ApJ, 620, L75
Alexander, D., et al., 2001, AJ, 122, 2156
Alexander, D., et al., 2002, AJ, 123, 1149
Barger, A., et al., 2002, AJ, 124, 1839
Blain, A., et al., 2002, PhR, 369, 111
Bouwens, R., et al. 2004, ApJ, 606, L25
Brandt, N., & Hasinger, G. 2005, ARA&A, in press (astro-ph/0501048)
Daddi, E., et al. 2000, A&A, 361, 535
Daddi, E., et al., 2003, ApJ, 588, 50
Dickinson, M., et al. 2003, ApJ, 587, 25
Dickinson, M., et al. 2004, ApJ, 600, L99
Franx, M., et al., 2003, ApJ, 587, L79
Gawiser, E., et al. 2005, ApJS, submitted
Kauffmann, G., et al., 1993, MNRAS, 264, 201
Koekemoer, A., et al., 2004, ApJ, 600, L123
Koekemoer, A., et al., 2005, in prep.
Kormendy, J., & Gebhardt, K. 2001 (astro-ph/0105230)
Labbé, I., et al. 2005, ApJL, submitted
McCarthy, P., et al. 2001, ApJ, 560, L131
Ouchi, M., et al. 2005, ApJ, 620, L1
Papovich, C., et al. 2004, ApJS, 154, 70
Stern, D., et al. 2005, ApJ (astro-ph/0410523)
Rix, H.-W., et al. 2004, ApJS, 152, 103
Rudnick, G., et al. 2003, ApJ, 599, 847
Shapley, A., et al. 2001, ApJ, 562, 95
Smail, I., et al., 2002, ApJ, 581, 844
Somerville, R., et al., 2004, ApJ, 600, L171
Steidel, C., et al. 1999, ApJ, 519, 1
Treister, E., et al. 2004, ApJ, 616, 123
van Dokkum, P., et al. 2003, ApJ, 587, L83
Yan, H., et al. 2004, ApJ, 616, 63

Observations Summary Table

Field	RA	DEC	Time
1	3:31:43.8	–27:36:17	2×12293
2	3:32:06.4	–27:36:17	2×12293
3	3:32:29	–27:36:17	2×12293
4	3:32:51.6	–27:36:17	2×12293
5	3:33:14.2	–27:36:17	2×12293
6	3:31:43.8	–27:41:17	2×12293
7	3:33:14.2	–27:41:17	2×12293
8	3:31:43.8	–27:46:17	2×12293
9	3:33:14.2	–27:46:17	2×12293
10	3:31:43.8	–27:51:17	2×12293
11	3:33:14.2	–27:51:17	2×12293
12	3:31:43.8	–27:56:17	2×12293
13	3:33:14.2	–27:56:17	2×12293
14	3:31:43.8	–28:01:17	2×12293
15	3:32:06.4	–28:01:17	2×12293
16	3:32:29	–28:01:17	2×12293
17	3:32:51.6	–28:01:17	2×12293
18	3:33:14.2	–28:01:17	2×12293

The 18 positions are the centers of 18 maps of 2×3 pointings (see above). The total exposure time for each map is 6 hours, split in two identical AORs of 3 hours each (as the total time per AOR, including overhead, may not exceed 6 hrs). The execution time of each 3hr AOR is 12293 seconds (including overhead). The total time request is $2 \times 12293\,\mathrm{s} \times 18$ pointings $= 122.9$ hours. This includes 108.0 hours science observations and 14.9 hours overhead. As explained above, the integration time *per pixel* will be ~ 3 hrs in all bands over the whole field.

The attached AOR is a single 12293s AOR for field 1.